Conf 910742--1

BNL--46378

DE91 015836

CHEMICAL CHARACTERIZATION OF AEROSOL PARTICLES BY RAMAN SPECTROSCOPY

I. N. Tang and K. H. Fung
Environmental Chemistry Division
Department of Applied Science
Brookhaven National Laboratory
Upton, NY 11973

June 1991

Accepted for presentation
in the poster session of the
7th International Conference on Surface and Colloid Science,
Compiegne, France
July 7-13, 1991
[WLT Registry Number 0665]

This research was performed under the auspices of the U.S. Department of Energy under Contract No. DE-AC02-76CH00016.

Introduction

Microparticles play a very important role in areas of atmospheric chemistry, combustion, interfacial science and others. Of particular importance is a knowledge of the chemical composition of these airborne particles. Until recently, much of the chemical information could only be obtained by analyzing sufficient quantities of particles collected on some substrate surfaces. In this paper, some of our recent work on chemical characterization of single particles by Raman spectroscopy are described.

Experimental Section

The spectrometer and the single particle levitation cell used in the Raman experiments are shown schematically in Figure 1. An electrostatically charged aerosol particle, 10-15 µm in diameter, is suspended in air at the null point of the cell by electrodynamic forces.(1,2) Dry or humidified nitrogen flows through the cell to provide the environment for particle phase transformation due to water vapor evaporation or condensation. A single spectral line (normally 4880 Å or 5145 Å) from an argon-ion laser, serves as the excitation source. The light scattered from the particle is collected with a condenser lens and imaged onto the entrance slit of a double monochromator with a resolution of 1.0 cm^{-1} (0.3Å). The photon detection system is an intensified diode array thermoelectrically cooled to -25°C for low dark current operation. For a typical spectrum, the total exposure time of the diode array is about 10 seconds, producing a total integrated Raman intensity about 6000 counts. Optical spectra are transferred by a DMA interface board to a PC and stored on floppy disks for later data analysis.

Results and Discussion

1. Solution droplets versus crystalline particles.

Ambient aerosols frequently contain large portions of a hygroscopic inorganic salts such as sulfates and nitrates, which are in the form of solution droplets or crystalline particles depending upon the relative humidity in the air.(3) It would, therefore, be desirable to develop a technique capable of not only chemical characterization but identifying the physical state of the particle. Since molecular vibrations are influenced by the medium surrounding the molecule and by its own motions in the liquid phase, the Raman effect is clearly suited for this purpose. A typical example is shown in Figure 2, where the Raman spectra are taken of a $NaNO_3$ particle (a) as a solution droplet at 1051 cm^{-1}, (b) during phase transformation, and (c) as a crystalline particle at 1067 cm^{-1}. The Raman shifts combined with line width differences between solid and liquid states provide a viable means for particle characterization.(4)

2. Salt mixtures versus mixed salts.

Ambient aerosols are far from being a single component system. When multicomponent electrolytes are present in a solution droplet, the free anions show characteristic Raman frequencies which are not affected by the presence of different cations. However, when the droplet becomes a solid particle under low humidity conditions, the chemistry of the system will operate to determine the outcome of the crystallization process. Simple salt mixtures, hydrated salts, or/and mixed salts may result.(5) Figure 3 shows the Raman spectrum of a particle composed of Na_2SO_4 and $NaNO_3$. While the characteristic Raman shifts for Na_2SO_4 at 995 cm^{-1} and $NaNO_3$ at 1067 cm^{-1} are clearly present, a new peak appearing at 1063 cm^{-1} is attributed to the presence of a mixed salt in the form of $NaNO_3 \cdot Na_2SO_4 \cdot 2H_2O$.

In Table 1, the Raman results observed for aerosol particles composed of some common sulfates and nitrates are given for chemical identification purposes. Here, the Raman shift given for each compound is the strongest vibration due to the symmetric stretching mode of the M-O bonds in the anion groups. Quantitative measurements by Raman spectroscopy are also possible from a determination of the relative peak intensities.(6,7) Figure 4 shows the linear relation between the Raman intensity ratio and the molar ratio for the $Na_2SO_4/NaNO_3$ system. The slope of the line represents the relative Raman scattering cross section for the given pair.(7)

3. Organic compounds.

Raman spectra have also been obtained for aerosol particles containing organic compounds including dioctyle phthalate, anthracene, and various aliphatic and aromatic acids. Because of the characteristic vibrations exhibited by the different functional groups, Raman spectroscopy is best suited for the identification of functional groups rather than individual compounds. Figure 5 shows the Raman spectra taken of suspended droplets of (a) oleic acid $CH_3(CH_2)_7CH = CH(CH_2)_7COOH$ and (b) myristic acid $CH_3(CH_2)_{12}COOH$. Both spectra reveal the presence of the CH_2 bending and twisting vibrations at 1460 and 1320 cm^{-1}, respectively, and the C-C stretching vibration at 1080 cm^{-1}. The C=C stretching vibration of oleic acid appears at 1660 cm^{-1}, which completely masks the very weak C=O stretching vibration at 1650cm^{-1}. In general, the Raman spectra of organic compounds are very complex in appearance but rich in molecular information. Numerous studies in the literature are devoted to the elucidation of molecular structures.

4. Resonance Raman Effect.

The compounds described above are colorless. They do not absorb the visible light including the 4880Å line used as the excitation source. The Raman effect for these compounds is spontaneous by nature with Raman scattering cross-sections in the order of 10^{-28} cm^2, which corresponds to a rather low sensitivity. However, the sensitivity may be greatly enhanced by using light at frequencies close to or within the absorption band of the compound. This is illustrated with Na_2CrO_4 particles, which are yellow crystals and has a very low absorbance for the blue laser light. The spectra obtained by using a mechanical chopper to reduce the heating effect are shown in Fig. 6, together with the 1067 cm^{-1} peak of $NaNO_3$ used as an internal standard. The measured relative cross-section, 20±3, is considerably higher than those of the common sulfates and nitrates given in Table II. For some compounds, an enhancement factor as large as 10^5 is possible due to the resonance absorption effect.

Conclusion

Raman spectra have been obtained for levitated single particles composed of some common inorganic salts or organic compounds. The results have demonstrated the feasibility of in situ chemical characterization of aerosol particles by this power spectroscopic technique.

References

1. Straubel, H. Naturwissenshaften 42, 506 (1955).
2. Wuerker, R. F., Shelton, H., and Langmuir, R.V. J. Appl. Phys. 30, 342 (1959).
3. Tang, I. N. J. Aerosol Sci. 7, 361 (1976).
4. Fung, K. H. and Tang, I. N. Appl. Opt. 27, 206 (1988).
5. Tang, I. N. and Fung, K. H. J. Aerosol Sci. 20, 609 (1989).
6. Fung, K, H. and Tang, I. N. J. Colloid Interface Sci. 130, 219 (1989).
7. Fung, K. H. and Tang, I. N. J. Appl. Spect. (in press).

Table I. Summary of Raman Shifts Observed for Crystalline Sulfates and Nitrates

Raman Shift, cm^{-1}	Chemical Identification
983	$(NH_4)_2SO_4 \cdot Na_2SO_4 \cdot 4H_2O$
992	$Na_2SO_4 \cdot 10H_2O$
995	Na_2SO_4
1043	NH_4NO_3 (rhombic)
1046	NH_4NO_3 (monoclinic)
1050	$2NH_4NO_3 \cdot (NH_4)_2SO_4$
1053	$2NH_4NO_3 \cdot Na_2SO_4$
1063	$NaNO_3 \cdot Na_2SO_4 \cdot 2H_2O$
1067	$NaNO_3$

Table II. Relative Raman Scattering Cross-Sections

Crystalline Compound	This Work	Literature
$NaNO_3$	1.0	1.0
NH_3NO_3	0.90 ± 0.03	—
Na_2SO_4	0.61 ± 0.05	0.67
$(NH_4)_2SO_4$	0.94 ± 0.02	0.65

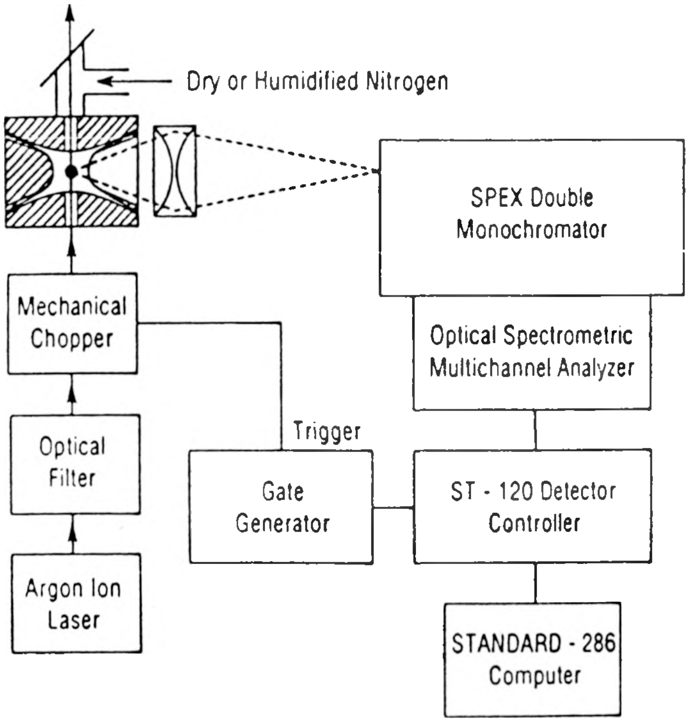

Figure 1

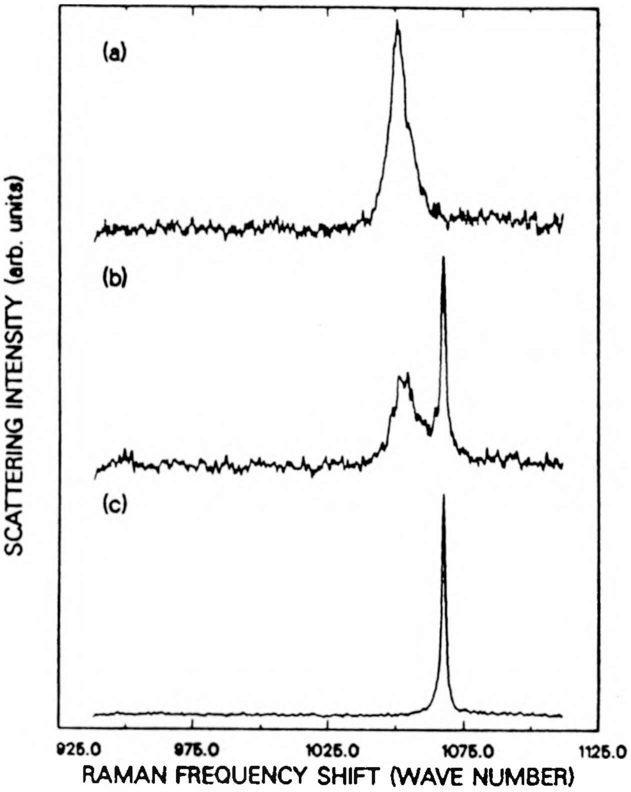

Figure 2

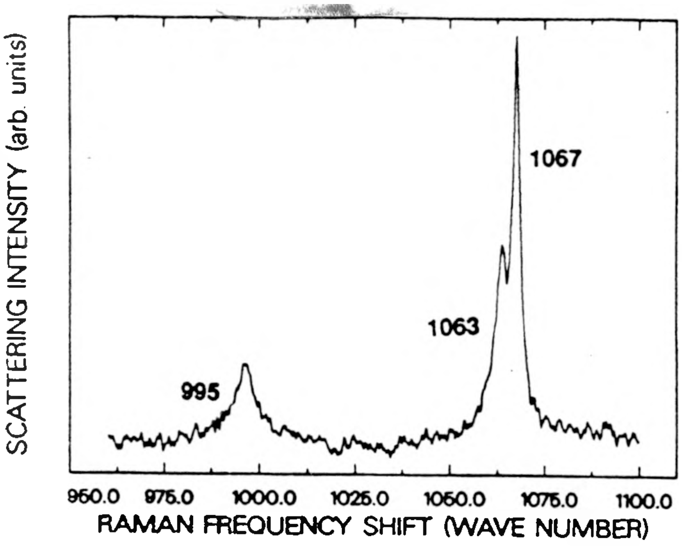

Figure 3

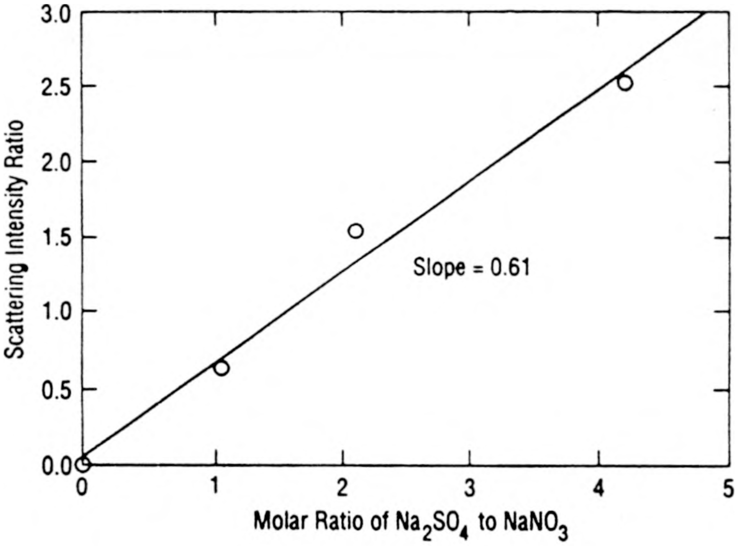

Figure 4

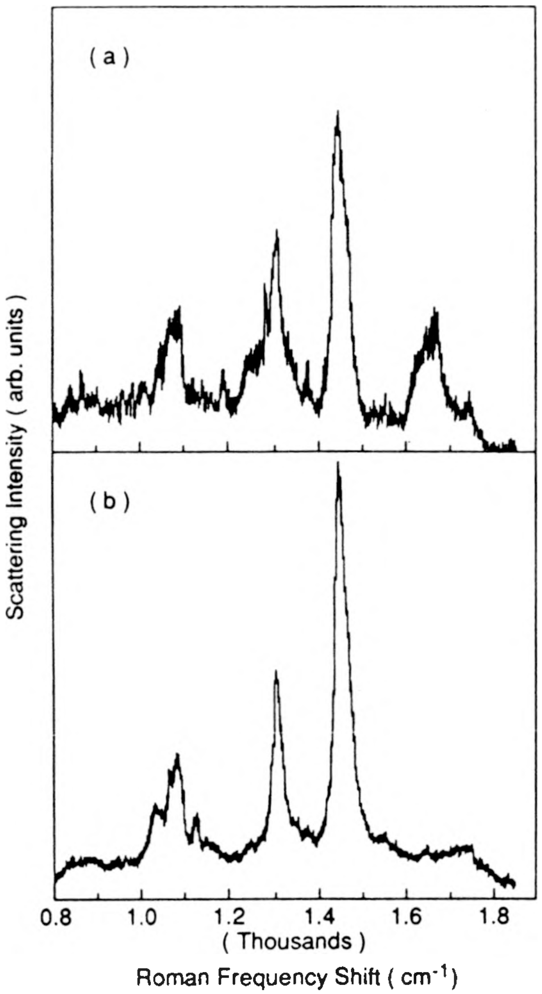

Figure 5

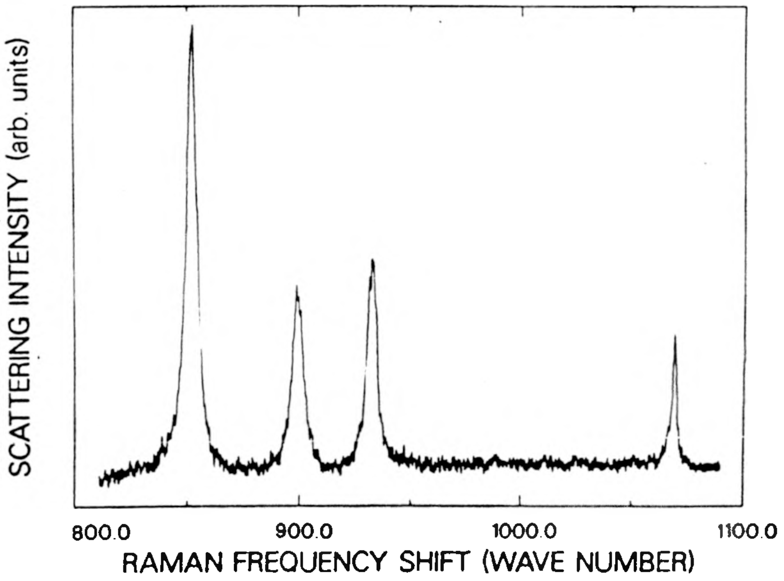

Figure 6